

Photo-oxidation of water sensitized by TiO₂ and WO₃ in presence of different electron acceptors

A. Mills and M.A. Valenzuela*

*Department of Pure & Applied Chemistry, University of Strathclyde,
Thomas Graham Building, 295 Cathedral Street,
Glasgow, G1 1XL, UK*

Recibido el 17 de septiembre de 2003; aceptado el 7 de octubre de 2003

The photo-oxidation of water is studied in presence of UV-light ($\lambda < 400$ nm) using titanium dioxide (TiO₂) and tungsten oxide (WO₃, micro- and nano-crystalline) semiconductors in presence of different sacrificial electron acceptors (SEA): Fe(NO₃)₂, Na₂S₂O₈, Ce(SO₄)₂, Co[(NH₃)₅Cl]Cl₂, AgNO₃, HgCl₂ and Cu(NO₃)₂. TiO₂ is 5 to 10 times more photoactive than WO₃ with reference to oxygen evolution. Ag ions are the best of the SEAs, for all the semiconductors tested in the photo-redox process. No oxygen evolution is observed when Hg²⁺ or Cu²⁺ ions are used as SEAs. The effect of high (10⁻² mol dm⁻³) and low (10⁻³ mol dm⁻³) SEA concentrations is also studied but no common trend is observed. Instead, each system (*i.e.*, SEA+H₂O+Semiconductor) exhibits a different behaviour and the results are rationalised in terms of the spectral and redox potential features of the system.

Keywords: Semiconductor photosynthesis; TiO₂; WO₃; water oxidation; electron acceptor.

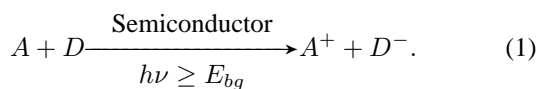
Se estudió la foto-oxidación del agua en presencia de luz UV ($\lambda < 400$ nm) empleando óxido de titanio (TiO₂) y óxido de tungsteno (WO₃, polvo y nanocrystalino) con diferentes aceptores de electrones (AE): Fe(NO₃)₂, Na₂S₂O₈, Ce(SO₄)₂, Co[(NH₃)₅ Cl] Cl₂, AgNO₃, HgCl₂ y Cu(NO₃)₂. En general, el TiO₂ presentó la mayor fotoactividad, produciendo entre 5 y 10 veces más oxígeno que el WO₃. En cuanto a las especies iónicas utilizadas en el proceso redox, los iones Ag⁺ fueron los más efectivos con los tres semiconductores. No se detectó la evolución de oxígeno cuando se utilizaron los iones Hg²⁺ y Cu²⁺. El efecto de la concentración de los AE no mostró una tendencia definida, si no que cada sistema (AE+H₂O+Semiconductor) tuvo un comportamiento distinto y los resultados se discutieron en función de sus características espectrales.

Descriptores: Semiconductores; TiO₂; WO₃; fotodescomposición del agua; aceptor de electrones.

PACS: 81.05.Hd; 82.50.Fv; 82.30.Lp; 82.65.Jv

1. Introduction

A great deal of semiconductor photochemistry is based on a relatively simple combination of processes, namely the initial photogeneration of an electron-hole pair and the subsequent reduction of an electron acceptor species (A) and concomitant oxidation of an electron donor (D) by the photogenerated electron and hole, respectively. If the change in Gibbs free energy for the overall reaction, *i.e.*, ΔG° , is positive for the uncatalysed process, then this is an example of semiconductor photosynthesis; and if ΔG° is negative, then it is an example of semiconductor photocatalysis [1]. A general semiconductor photosensitisation reaction can be summarised by

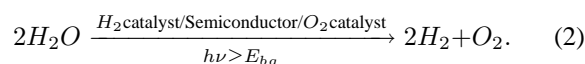


In such a photosensitisation reaction, at the end of the photoredox reaction, the semiconductor remains unchanged [1-6].

For many years titanium dioxide (titania) has been the practical photocatalyst of choice amongst researchers for a variety of reasons including: its high stability and oxidising power [7-8]. Powders and thin films of titania can be used as semiconductor photocatalysts to photodegrade a wide range of organic and inorganic chemicals in air and water [9-11]. Other applications include: the elimination of microorgan-

isms such as bacteria [12-14], viruses [15], cancer cells [16] the reduction of trace heavy metals [17] and the splitting of water [18].

The photoproduction of hydrogen and oxygen by splitting water has been studied by many research groups since the early 1970s. [19-36]. The basic process may be summarised as follows:



The water splitting reaction is a two-electron process per molecule of hydrogen generated, with $\Delta G_{298}^\circ = 237.7$ kJ mol⁻¹. This thermodynamically unfavorable reaction can be made to proceed by semiconductor photosynthesis, where the semiconductors are: TiO₂, SrTiO₃, and CdS. The system often requires an H₂ catalyst, usually Pt, since the overpotential for water reduction is very large on most semiconductor materials and cannot be overcome by the photogenerated electrons. Similar arguments are made for the inclusion of an oxygen catalyst, such as RuO₂, into the system, although this is often not crucial as the photogenerated holes are usually sufficiently oxidising as to overcome the appreciable overpotential (+0.8V) for water oxidation [35].

In terms of the energetics, the standard redox potentials of the couples, H⁺/H₂ and O₂/H₂O, must be located in a

narrower range than that covered by the redox potentials associated with the photogenerated electron, *i.e.*, the conduction band (CB), and the photogenerated hole, *i.e.*, the valence band (VB), in order to carry out the photocleavage of water. The positions of the redox potentials of the H^+/H_2 and O_2/H_2O couples, along with those of the CB and VB for a series of popular semiconductor photosensitisers are illustrated in Fig. 1. A brief inspection of the data in this diagram shows that, whereas only silicon is thermodynamically incapable of oxidising water to oxygen at pH 0, the semiconductors, SnO_2 , Fe_2O_3 and WO_3 are unable to reduce water to hydrogen. The data in Fig. 1 indicates that a number of semiconductors are capable thermodynamically of splitting water, although, in practice, this number is very limited for a variety of reasons, including: low photostability, low photoactivity and high overpotentials. Certainly, the most difficult of the two processes associated with water splitting is the photo-oxidation of water, since many semiconductors, *e.g.* CdS and CdSe, undergo the alternative oxidative process of photoanodic corrosion.

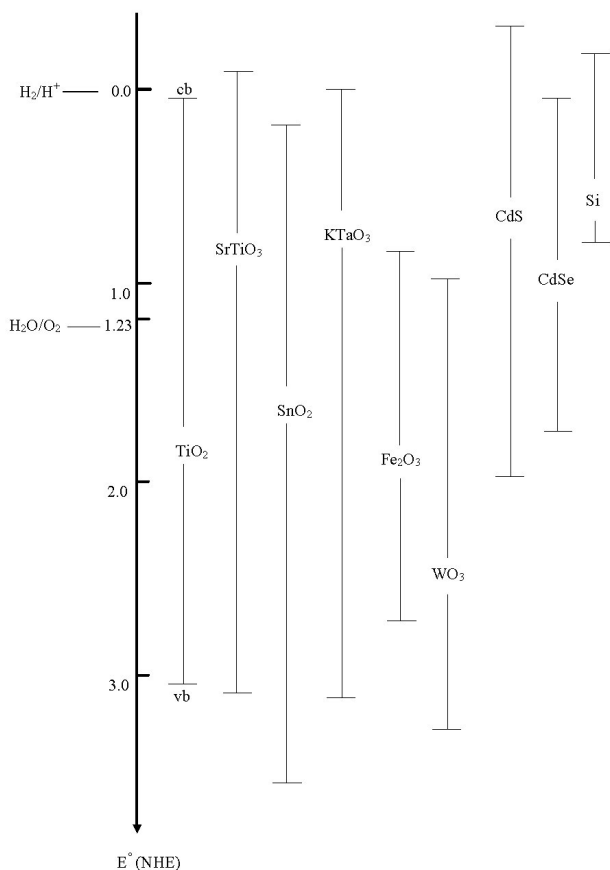
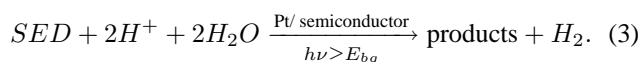


FIGURE 1. Redox potentials (at pH0) of the valence band (VB) and conduction band (CB) of various potential water-splitting semiconductors, including WO_3 and TiO_2 . For reference, the redox potentials of the O_2/H_2O and H^+/H_2 redox couples have been included.

The photocleavage of water is a difficult process, involving as it does the formation of many chemical intermediates which are likely to react with each other and so short-circuit the overall process. It is no surprise, therefore, given its difficulty, to note that reaction (2) has been and is the subject of much controversy. Certainly, the main problems to be solved with this photoreaction are its very low quantum yields, associated with the thermal back reactions, and the fact that most systems developed to date utilise UV rather than visible light [34]. However, interest in water splitting continues and those involved suggest that forcing conditions, such as reduced pressures and elevated temperatures, are needed, to help eliminate back reactions (due to the accumulation of H_2O and O_2) by stripping them out before they can react [1,37].

As indicated earlier, the easier half of the water splitting photosystem, *i.e.*, H_2 production, has been much more studied than the photo-oxidation of water to O_2 . Indeed, it is well known that ultra-bandgap irradiation of systems containing: TiO_2 , CdS and a number of other semiconductors can effect the photoreduction of water, if alcohols, EDTA, sulfite ions, glucose or other compounds are used as the sacrificial electron donor (SED) [18,35]. The basic overall process can be summarised as follows:



In almost all cases a PGM catalyst, such as Pt, is needed in the system, usually on the surface of the semiconductor particles, to help mediate the reduction of water.

As for oxygen evolution, TiO_2 , WO_3 , CeO_2 and mixed TiO_2 - WO_3 photocatalysts in presence of Fe^{3+} , $[PtCl_6]^{2-}$, Ag^+ or Ce^{4+} as sacrificial electron acceptors, *i.e.*, SEAs, have been shown to function quite well as examples of water oxidation photosystems [35]. The photogenerated hole on titania and WO_3 (the two most commonly used semiconductors photosensitisers) is so oxidising, *i.e.*, $E_{VB} \gg E^\circ(O_2/H_2O)$, that an oxygen catalyst seems not to be needed. Despite this fact, the use of an oxygen catalyst, such as RuO_2 , to facilitate the overall semiconductor-sensitiser photo-oxidation of water to O_2 , remains popular. In such systems, the semiconductor-sensitised photocatalytic oxidation of water by a SEA can be expressed by the following simple reaction process:

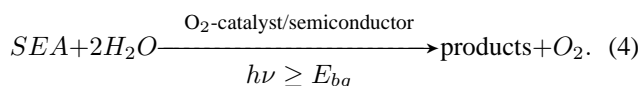


Figure 2 summarises the basic electron transfer processes associated with the semiconductor-sensitised photo reduction (reaction 3), oxidation (reaction 4), and cleavage of water (reaction 2).

Although a number of studies of reaction (4) have been conducted in the past using a variety of different individual sacrificial electron acceptors, a more comprehensive study of the efficacy of such SEAs has been lacking. Thus, in this paper, the results of a study of the effectiveness of a number of

different SEAs in photoreaction (4) are reported in which the semiconductors are TiO₂ (P25) and WO₃, with the latter in a microcrystalline and nanocrystalline form.

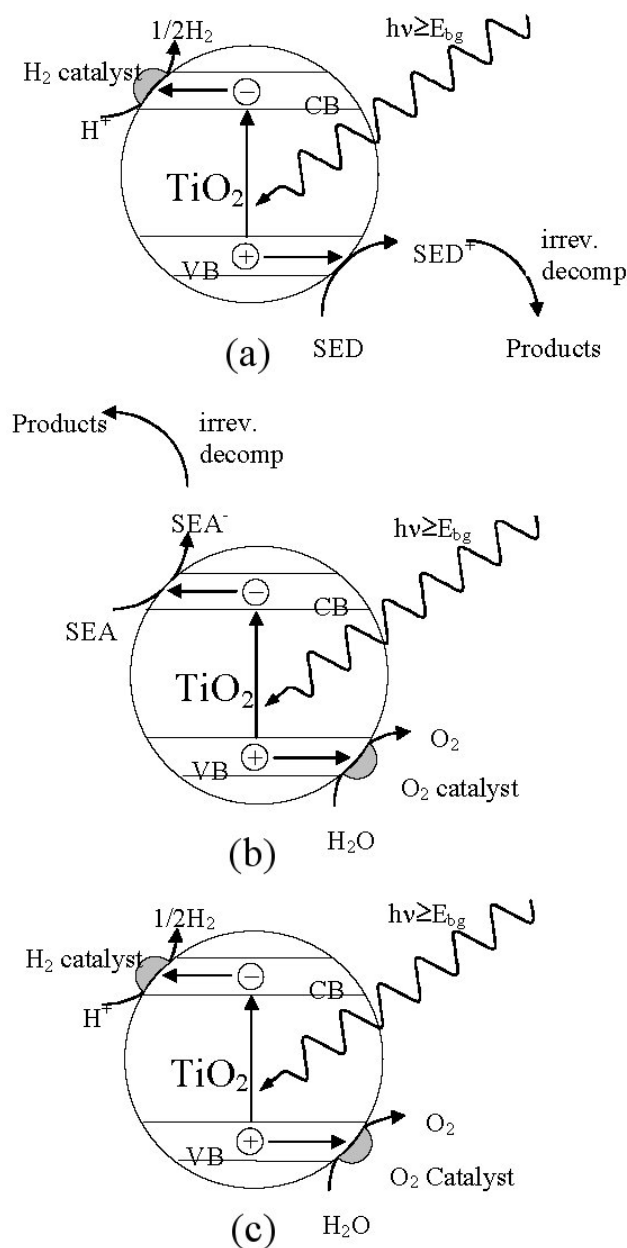


FIGURE 2. Schematic illustrations of the electron energetics associated with: (a) the photoreduction of water by a sacrificial electron donor (SED) sensitized by semiconductor particles which have surface deposits of a hydrogen catalyst, such as Pt; (b) the photooxidation of water by a sacrificial electron acceptor (SEA) sensitized by semiconductor particles with surface deposits of an oxygen catalyst, such as RuO₂, (note: in practice often the O₂ catalyst is omitted) and (c) the photocleavage of water, sensitized by semiconductor particles with surface deposits of a hydrogen catalyst and an oxygen catalyst.

2. Experimental

2.1. Materials

The TiO₂ used throughout this work was P25 TiO₂ supplied by Degussa-Huels. The WO₃ micro and nanocrystalline were obtained from Aldrich Chemicals. The micro WO₃ powder is yellow-green, dense and coarse and forms aggregates in solution that are much greater than a micron in size and, as such, very readily settle. In contrast, nano WO₃ powder is light and fine, although still yellow-green in appearance, and forms submicron aggregates in solution that do not readily settle. The SEAs: Fe(NO₃)₃·9H₂O, Na₂S₂O₈, AgNO₃ and HgCl₂ were supplied by Aldrich Chemicals. Ce(SO₄)₂ and Cu(NO₃)₂·3H₂O were purchased in AnalaR form from Aldrich Chemicals. The [Co(NH₃)₅Cl]Cl₂ complex was obtained from Alfa Aesar. All materials were used as received. Solutions containing Fe³⁺ or Ce⁴⁺ were prepared from the appropriate salts mentioned above using aqueous 0.01M and 0.5 M H₂SO₄, respectively, as solvent. Solutions containing Ag⁺ or Cu²⁺ ions were prepared from their salts using aqueous 0.01M HNO₃ as the solvent. Mercury chloride solutions were prepared using aqueous 0.01M HCl as the solvent. The use of acidic conditions in making up solutions of these metal ions were employed in order to minimise or eliminate problems due to metal ion hydrolysis (vide infra). Sodium persulphate and the [Co(NH₃)₅Cl]Cl₂ solutions were prepared using just water as the solvent. In all cases the water used to make up the solutions was doubly distilled. The nitrogen used to purge the solutions before each irradiation was obtained from BOC and was free of O₂.

2.2. Methods

UV-VIS absorption spectra were recorded using a Helios β UV-VIS spectrophotometer (Thermo Spectronic). Diffuse reflectance spectra were recorded using a Perkin Elmer Lambda 20 UV-VIS spectrophotometer with a diffuse reflectance attachment. Details of the irradiation system have been reported elsewhere [38,39], but, in brief, the photoreactor comprised two half cylinders, each containing six 8 W Black Light UVA lamps set against a half-cylinder aluminium reflector. Each of the lamps (Coast Air®) emitted a broad range of UVA light, typically 320-390 nm, with λ_{max} (emission) = 355 nm. The photochemical reaction vessel used in this work comprised a 60cm³ thermostatted glass vessel with an oxygen electrode in its base (i.d. 4 cm). The concentration of dissolved oxygen in the reaction vessel was measured using this oxygen electrode (purchased from Rank Brothers, UK), a detailed description of which is given elsewhere [40]. Figure 3 is a labelled photograph of the irradiation system opened up to reveal the glass photoreactor with the oxygen electrode in its base, set on a magnetic stirrer and the two halves of the photoreactor. In practice the two halves of the photoreactor, containing the UV-lamps, are pushed together, with the photoreaction pressed in its centre, before the start of any irradiation. The reaction solutions under test were

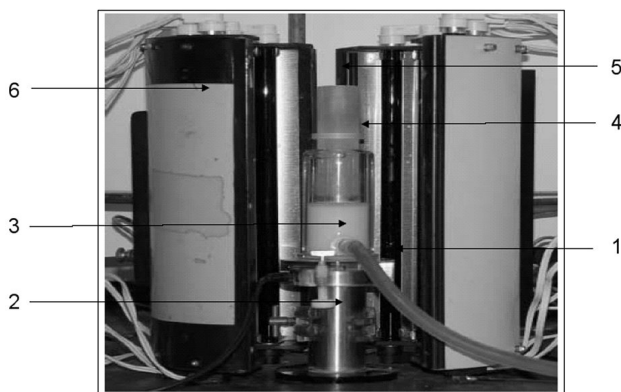


FIGURE 3. Labelled photograph of the irradiation system comprising: a photo reactor, and photoreaction vessel with an O₂ electrode set in its base (1) oxygen electrode (2) magnetic stirrer (3) glass photoreaction vessel (4) plunger (5) black light lamp (5) half cylinder.

placed in the O₂ electrode, prior to irradiation and stirred and thermostatted at 25°C. Before each experiment the solutions (typically comprising x mg of semiconductor photocatalyst, where $x = 12.5$ (TiO₂), 25 (WO₃ nano) or 50 (WO₃ micro), dispersed in 25 ml of the SEA solution under test, after sonication for 15 min in an ultrasonic bath to disperse the semiconductor powder and transfer to the photochemical reaction vessel, were purged with oxygen-free nitrogen prior to illumination. After purging, the plunger in the top of the reaction vessel was pushed down in order to expel all the headspace above the solution. The photoreaction was then initiated by turning on the lamp of the photoreactor.

3. Results and discussion

3.1. Spectral features of the semiconductors

Figure 4 shows the % reflectivity, as measured by diffuse reflectance, as a function of wavelength for the series of semiconductor samples used in this work. This plot is similar to that of the transmittance spectrum of a substance, and, thus, from the data in Fig. 4, it can be seen that TiO₂ absorbs most strongly in the near UV ($\lambda < 400$ nm), whereas the two WO₃ powders absorb strongly both in the UV and visible wavelength regions. Using the results illustrated in Fig. 4, the absorption onset wavelengths were estimated as 405, 459 and 474 nm, for TiO₂, WO₃ micro powder and WO₃ nanopowder, respectively. These experimental results were used to calculate the band gap energies for the three powders, using the formula E_{bg} (eV) = $1240/\lambda_{t\text{extonset}}$ (in nm), which were as follows: 3.06, 2.70 and 2.61 eV. These values are consistent with those reported by others [41]. In particular, although the bandgap of the two WO₃ powders was estimated to lie in the region 2.6-2.7eV, and the value for bulk single-crystal WO₃ is reported as 2.7-2.8eV, others have also reported it as low as 2.6eV for WO₃ powders [41]. Not surprisingly, the measured specific surface area (using the BET method) was significantly bigger in the case of WO₃ nanopowder (25 m²/g)

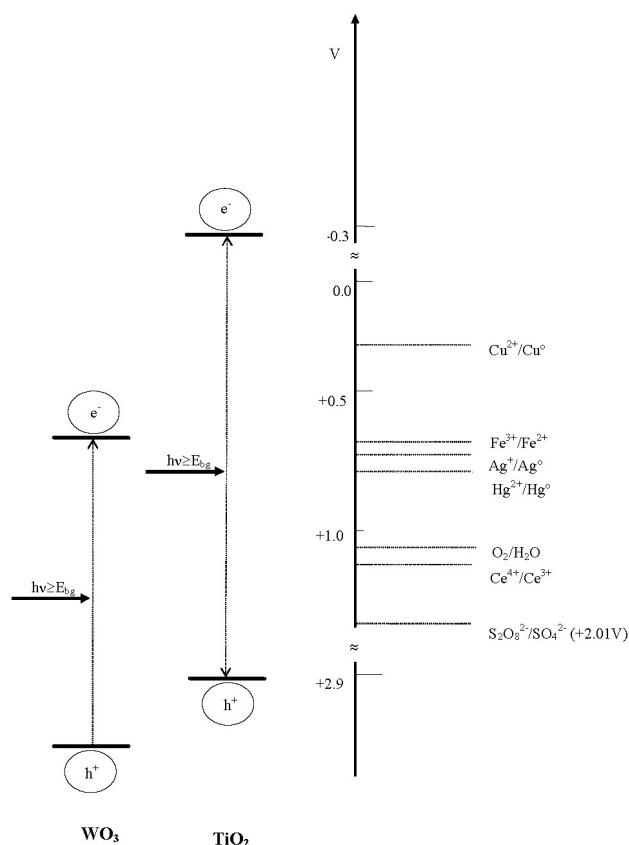


FIGURE 4. Illustration of the standard redox potentials at pH=0 of the valence band (VB) and of the conduction band (CB) of WO₃ and TiO₂. The redox potentials of the O₂/H₂O and various relevant redox couples associated with the sacrificial electron acceptors under test are also illustrated.

compared with the microcrystalline WO₃ conventional powder (5m²/g). Assuming in both cases the powder particles are spherical, and given that the specific surface area of such an ideal powder = $6/\rho d$, where ρ is the density of WO₃ (7.3×10^6 g/m³) and d is the diameter of the spherical powder particles, then the size of the powder particles can be estimated as 0.16 μ m and 33nm for the micro and nano WO₃ powders. Note the size of the nano WO₃ powder particles is similar to those of the ubiquitous non-porous Degussa P25 TiO₂ powder, a 70:30 mixture of anatase and rutile, also used in this work, which has a specific surface area of 50 m²/g and average particles size of ca. 31nm.

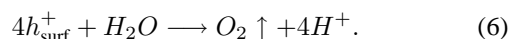
3.2. Photoreaction energetics

Illumination of a semiconductor, such as TiO₂ or WO₃, with ultra bandgap light generates an electron-hole pair. The subsequent fate of this pair is key to the overall photoactivity exhibited by the semiconductor photocatalyst. In most cases, including TiO₂ and WO₃, the electron-hole pairs recombine, either in the bulk of the particles where they were created, or at the surface of the semiconductor. As a consequence, semiconductor photochemistry is usually inefficient in its use of

photons, *i.e.*, most systems exhibit low quantum yields, typically of the order of 1%. If the photogenerated electrons and hole are able to reach the surface of the particle they were generated in, then they can react with substances adsorbed at the surface. In this work different sacrificial electron acceptors have been added to the reaction solution, comprising dispersed particles of semiconductor, so as to react with any surface photogenerated electrons, *i.e.*,



Several of the SEAs used in this work, such as Hg²⁺, Cu²⁺ and S₂O₈²⁻, are associated with a multi-electron redox couple. In such examples, as with single electron redox couples, the initial electron-transfer step, *i.e.*, reaction (5), is usually considered the rate determining step. With the rapid removal of the photogenerated electrons, via reaction (5), the photogenerated holes will accumulate at the surface of the semiconductor. In the cases of WO₃ and TiO₂ the photogenerated holes are sufficiently oxidising that they are able to oxidise water to oxygen, *i.e.*,



However, there is also a possibility that the photogenerated holes may oxidise SEA⁻ to SEA and so short-circuit the overall process. This is likely to be a problem if SEA⁻ is stable and adsorbed strongly on the surface of the semiconductor. If, however, reactions (5) and (6) do proceed efficiently, and there are no 'short-circuiting' back reactions, then the overall photo-oxidation by the sacrificial electron acceptor of water to oxygen, as summarised by reaction (4), will be effected. Obviously for this reaction to be efficient the reaction energetics must be favourable. The change in Gibbs free energy for the water oxidation reaction (6) can be summarised as follows:

$$\Delta G = -nF(E_{VB} - E^\circ(\text{O}_2/\text{H}_2\text{O})), \quad (7)$$

where *n* is the number of electrons transferred (*n* = 4 for water oxidation) and *E_{VB}* is the redox potential of the photogenerated holes in the valence band of the semiconductor. The positions of the redox potential, *E_{VB}*, for WO₃ and TiO₂ and *E*[°](O₂/H₂O) at pH 0 are given in Fig. 5, from which it is quite clear that *E_{VB}* ≫ *E*[°](O₂/H₂O) for both WO₃ and TiO₂ and, therefore, Δ*G* for reaction (6) is negative and quite large, and thus the process is thermodynamically feasible.

The change in Gibbs free energy for the SEA reduction reaction (5) can be summarised as follows:

$$\Delta G = +nF(E_{CB} - E^\circ(\text{SEA}/\text{SEA}^-)), \quad (8)$$

where *E_{CB}* is the redox potential of the photogenerated electrons in the conduction band of the semiconductor. As before, the positions of the redox potentials for *E_{CB}* for WO₃ and TiO₂ and the standard redox couples associated with each SEA are illustrated in Fig. 5. Note: the latter potentials are not usually quite the same as that of *E*[°](SEA/SEA⁻) for the multi-electron redox couples. Indeed, although the standard redox potentials of all the multi-electron redox couples are known, quite often the redox potentials for the one-electron couples, *i.e.*, *E*[°](SEA/SEA⁻), are not, as in the case of persulfate. However, in spite of this, a rough guide to the feasibility of reaction (5) can be gleaned from a brief inspection of the data in Fig. 5 and the application of Eq. (8). Thus, from this data, it is clear that thermodynamically all the SEAs chosen are able to react with the photogenerated electrons on TiO₂, since in all cases *E_{CB}* < *E*[°](SEA/SEA⁻) and; therefore, Δ*G* is negative. In contrast, it is clear that, in terms of thermodynamics, the condition for feasibility, *i.e.*, *E_{CB}* < *E*[°](SEA/SEA⁻), is not satisfied by the Cu²⁺ SEA, at least when WO₃ is used as the semiconductor sensitizer.

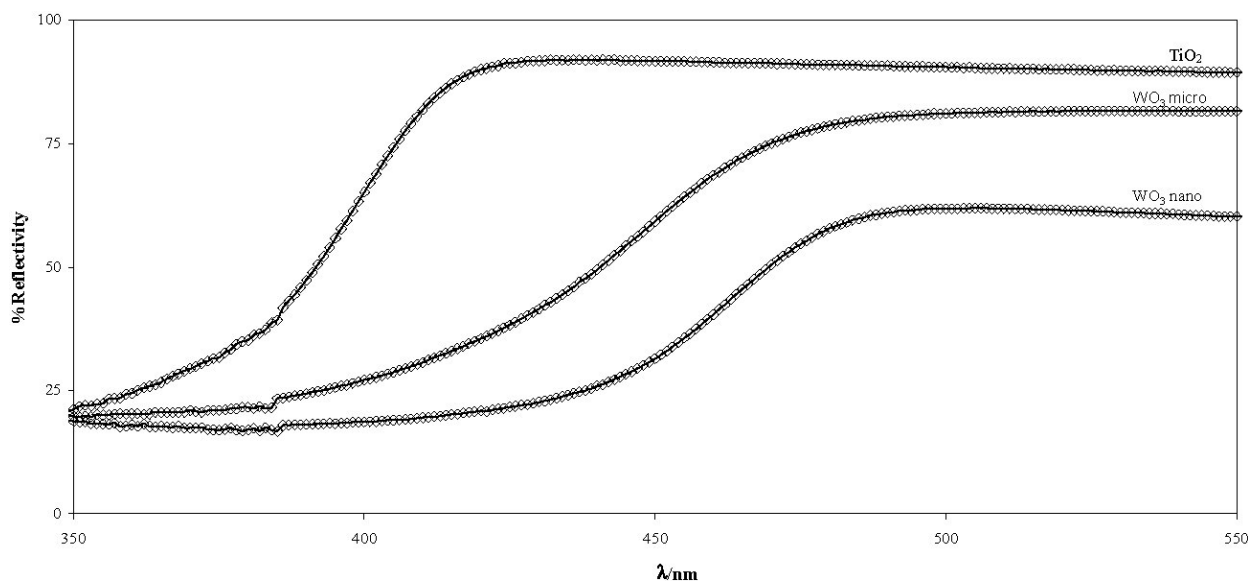


FIGURE 5. % reflectivity UV-VIS diffuse reflectance spectra of the different semiconductor photocatalysts used in this work; from top to bottom: TiO₂, WO₃, (nano) and WO₃ (micro), respectively.

3.3. Spectral features of the SEA compounds

Figure 6 shows the UV-VIS spectra of the in aqueous solutions of the SEAs at the two concentrations used in this work, namely: 10^{-2} and 10^{-3} mol dm $^{-3}$. The Fe $^{3+}$ and Ce $^{4+}$ ions absorb strongly at around 400 and 450 nm, respectively, and at all wavelengths below these values whereas the [Co(NH $_3$) $_5$ Cl] $^{2+}$ complex absorbs in the visible region (maximum at around 500 nm) as well as in the UV (400 nm). The S $_2$ O $_8^{2-}$, Ag $^+$, Hg $^{2+}$ and Cu $^{2+}$ SEAs have similar spectral characteristics, all absorbing in the far UV, *i.e.*, at ca. 250 nm at high concentrations and at slightly lower wavelengths at the lower concentration.

An appreciation of the spectral characteristics of the different SEAs tested is important, since any strongly UV or visible absorbing solution additive, such as an SEA, can act as an effective screen to ultra bandgap photons and so prevent their absorption to a significant extent by the semiconductor. Obviously, the potential problem of screening is more significant the more UV absorbing and concentrated the additive, especially for the only UV-absorbing semiconductors, such as titania.

In a typical experiment 12.5 mg of Degussa P25 TiO $_2$ were dispersed in an aqueous solution (25ml), comprising 10^{-3} mol dm $^{-3}$ of silver nitrate, and placed in the thermostatted, glass photoreaction vessel, set in the base of which was an oxygen electrode. Upon UV illumination of this sys-

tem, with twelve 8W blacklight lamps, the evolution of dissolved oxygen was measured by the oxygen electrode. The recorded variation of the output of the oxygen electrode versus time profiles for this semiconductor and the two different WO $_3$ powders (25 mg (WO $_3$ nano) and 50 mg (WO $_3$ micro), dispersed in 25 ml of the SEA solution) are illustrated in Fig. 7.

The output of an oxygen electrode is directly proportional to the level of dissolved oxygen. Thus, using air-saturated water as a calibrant [O $_2$] = 2.5×10^{-4} mol dm $^{-3}$, it is a simple task to convert this output into a plot of dissolved oxygen concentration versus time. Thus, from the data in Fig. 7, it is clear that silver ions function very well as SEAs. Presumably the difference in redox potential of the photogenerated conductance band electrons and that of the E $^\circ$ (Ag $^+$ /Ag) couple is the underlying cause for the much greater efficacy of Ag $^+$ ions as a SEA when titania is used as the semiconductor as compared with to the two WO $_3$ powders. Another cause for this difference in rate of oxygen evolution is the much greater specific surface area of TiO $_2$, compared to that of the two tungsten powders. Certainly there was a noticeable difference in the nature of the dispersion, with the fine, nano powder forming much better dispersions than the coarser, microcrystalline WO $_3$ and this effective difference in surface area and ability to form a stable dispersion is the likely major cause for the difference in photocatalytic activity exhibited by the two WO $_3$ powders, as illustrated by the data in Fig. 7.

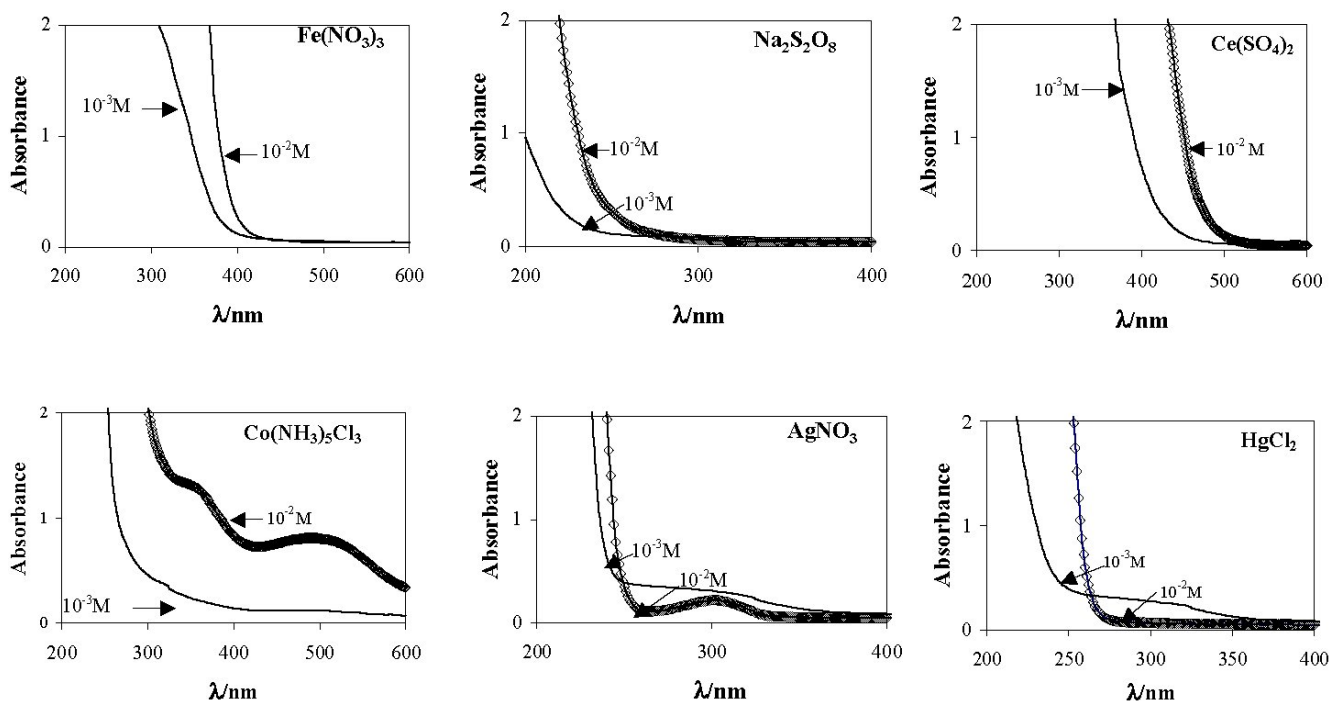


FIGURE 6. UV/VIS absorption spectra of aqueous solutions of the different SEAs used in this work.

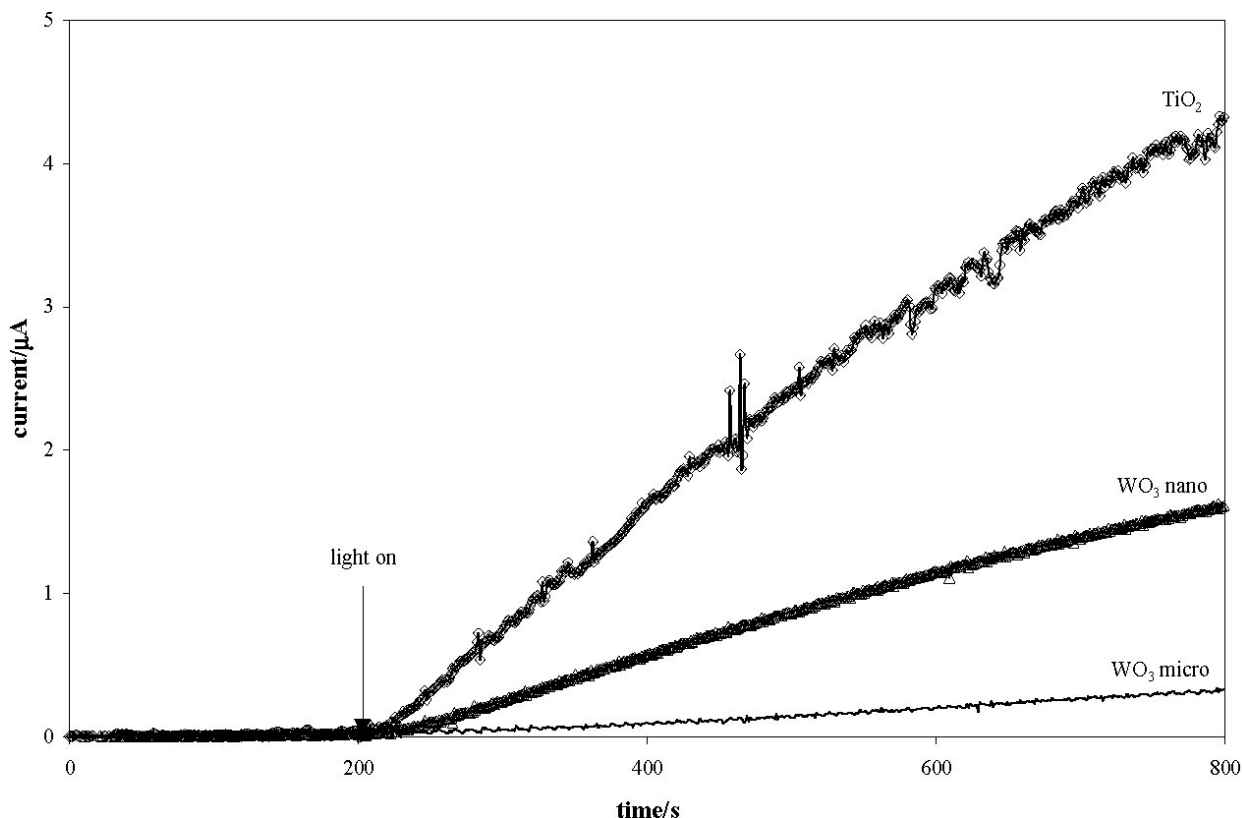


FIGURE 7. Measured dissolved [O₂] versus illumination time profiles, made using a 10⁻³ M aqueous solution of silver nitrate as SEA and (a) TiO₂, (b) nano WO₃ and (c) micro WO₃, powders as the semiconductor (12.5 mg (TiO₂), 25 mg (WO₃ nano) and 50 mg (WO₃ micro), dispersed in 25 ml of the SEA solution).

Using the above general procedure the following SEAs were tested, using TiO₂ and the micro and nanocrystalline WO₃ powders as semiconductor photocatalysts for reaction (4): Hg²⁺, Cu²⁺, Ag⁺, Ce⁴⁺, Fe³⁺, S₂O₈²⁻ and Co(NH₃)_s(Cl²⁺). In the cases of Hg²⁺ and Cu²⁺, no oxygen evolution was observed with any of the semiconductors tested. As previously noted, the lack of any oxygen evolution for the WO₃/Cu²⁺ systems is not surprising on energetic grounds. Given the favourable energetics of reaction (4), especially for the combination of TiO₂ and Cu²⁺ and Hg²⁺, the lack of any reaction appears surprising initially. However, similar results, based on TiO₂, have been reported by others and are attributed to the relative easy of reoxidation of the reduced forms of these ions, *i.e.*, Cu⁺, Hg⁺, Cu and Hg by the photogenerated holes [17]. Other work showed that whilst the reaction of Hg²⁺ ions to Hg could be achieved using TiO₂ as the photocatalyst and methanol, rather than water, as the source of electrons, the finely-divided Hg deposited was very rapidly reoxidised by air. Thus, as with many heterogeneous photocatalytic reactions, reaction (4) although on first inspection apparently very simple, can be, in fact, much more complex, especially if highly reactive intermediates that adsorb or deposit on the surface of the semiconductor photocatalyst are involved.

Histogram plots of the observed initial rates of oxygen evolution per gram of photocatalyst for reaction (4), using TiO₂ and micro and nanocrystalline WO₃ as the semiconductor photocatalyst, and the other SEAs tested, at two different concentrations, are illustrated in Fig. 8. As noted before, and illustrated in Fig. 7, Ag⁺ ions are a very effective SEA at 10⁻³ and 10⁻² mol dm⁻³. However, it is surprising to note that the rate of water oxidation via reaction (4) is much slower at [Ag⁺] levels of 10⁻² compared to 10⁻³ mol dm⁻³ when the microcrystalline WO₃ powder is used as the semiconductor photocatalyst. Why this is so is not clear, although there is some evidence to suggest that Ag⁺ ion-adsorption induced particle aggregation may be responsible. Further work is required to clarify the situation.

From previous discussions of the energetics of reaction (4) it is fairly clear that Co(NH₃)_sCl²⁺ is not expected, from thermodynamics at least, to be an effective SEA for either of the two WO₃ powders given the poor reducing power of their photogenerated electrons ($E_{CB}(\text{WO}_3) = +0.4\text{V}$ vs NHE) and the low redox potential of the Co(NH₃)_sCl²⁺/Co(NH₃)_sCl⁺ couple. In contrast, as illustrated by the results in Fig. 8, TiO₂, with its much more reducing conduction band ($E_{CB}(\text{TiO}_2) = 0.1\text{V}$ vs NHE), is able to sensitise reaction (4), using Co(NH₃)_sCl²⁺ as the SEA, especially when the latter is at a high concentration.

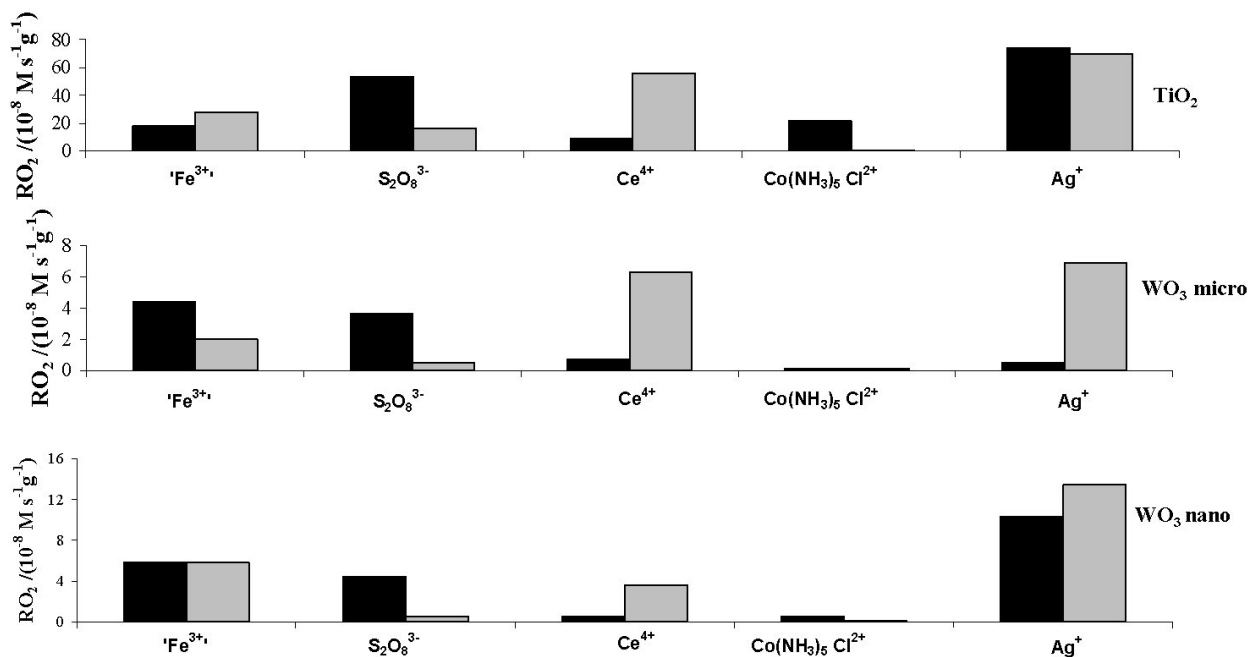
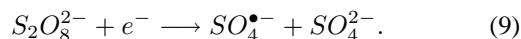


FIGURE 8. Histogram plots of the measured rates of the photo-oxidation of water per gram of photocatalyst using various different SEAs and sensitised by TiO₂, micro WO₃ or nano WO₃ semiconductors.

Based on energetic arguments, one of the best SEAs tested should be Ce⁴⁺ ions and one might expect that the higher the concentration the faster the rate of oxygen photoevolution via reaction (4) for all the semiconductors tested using this SEA. However, contrary to these expectations, the results illustrated in Fig. 8 show that ceric ions appear to act as a poor SEA at high (10⁻² mol dm⁻³) concentrations, but are much more effective at lower concentrations (such as 10⁻³ mol dm⁻³). The cause for this behaviour is the UV screening action of ceric ions, which is very effective at high concentrations, but much less so at lower concentrations, as illustrated by the UV/VIS spectra of the ceric ion solution in Fig. 6. Thus, when considering the efficacy of a SEA it is important to take into account a number of factors, including the energetics of the process and the bandgap screening action of the SEA.

As illustrated by the UV/VIS spectra of the two persulfate solutions used as SEAs in this work (see Fig. 6), UV-screening is not a problem with S₂O₈²⁻ ions. Indeed, in terms of energetics, S₂O₈²⁻ is the most favourable of all the SEAs tested, exhibiting, as it does a redox potential of 2.08 V vs NHE. It is no surprise, therefore, to note from the data illustrated in Fig. 8 that S₂O₈²⁻ proved an effective SEA for all the semiconductors tested and the higher its concentration the greater the rate of oxygen evolution. In fact, what is slightly surprising, given its lack of UV-screening and very favourable energetics, is that the observed rate of water photo-oxidation is not any faster than most of the other, less-favourable, SEAs tested. Indeed, Ag⁺ ions appear a better SEA than S₂O₈²⁻ ions, despite the much lower oxidation potential of the Ag⁺/Ag couple compared to that of the S₂O₈²⁻/SO₄²⁻ couple. However, persulfate is a recognised

curiosity as an oxidising agent, often working very slowly in this role, except in the presence of a catalyst, such as the silver ion [42]. Its mechanistic action in such oxidation reactions is complex but it is usually suggested that the initial step involves formation of the highly reactive sulfate radical SO₄^{•-}, *i.e.*,



In reaction (4), where persulfate is the SEA, it appears likely that SO₄^{•-} radicals are produced as the intermediate. The slightly lower than expected rate of photo-oxidation of water, via reaction (4), observed for all the semiconductors tested may well be due to the high reactivity of this radical intermediate which results in a tendency to react with the photogenerated holes, so short-circuiting the overall reaction. Interestingly, additional work carried out on the same sacrificial system at high pH (pH 13 instead of pH 6.5) produced a marked (6 fold) increase in rate, possibly due to an increase in the stability of the SO₄^{•-} radical and a lower overpotential for water oxidation [43].

Finally, ferric ions at pH 2 as a SEA in reaction (4) proved quite effective, although, like Ce⁴⁺ ions, the rate was found to decrease at high concentrations due to a UV-shielding effect (see Fig. 8). The use of ferric ions as a SEA for reaction (4) has been well-studied for both TiO₂ and WO₃ as semiconductor photosensitisers [41, 44-46]. However, often in such work researchers forget to acknowledge that Fe(III) ions only exists in the form of the pale purple hexaquo ion at ca. pH 0 [42]. At pH's > 0, the ferric ion hydrolyses and forms complexes. Indeed at pH > 3.5 ferric ions form a gelatinous red-brown precipitate that contains Fe(OH)₃ and many,

undefined polymeric species. Thus, the highly UV absorbing nature of the solution of ferric sulfate (pH2) used in this work does not comprise Fe³⁺ ions but rather a complex mixture of hydrolysed Fe(III) species. The colour and composition of this solution is fairly stable but at higher pH's (*i.e.* pH>2) it changes with time, becoming more UV-absorbing and orange in appearance over a period of time that can be minutes, hours or days; obviously the higher the pH the faster the hydrolysis process. This effect is even greater at higher pH's. In order to ensure the ferric solutions used in this work were of the same, albeit partially hydrolysed, composition the solutions were made up fresh on the day and used shortly afterwards. Previous reports by others of rates of oxygen evolution based on studies of reaction (4) where ferric ions were used as the SEA and the pH adjusted to pH>2 and used at an undefined time later are of little value since not only is the composition of the SEA not known, but the work cannot be repeated since, at these pH's, the composition of the SEA changes as a function of time [45]. The same problem is also encountered in work carried out using Ce⁴⁺ ions, since these ions are also rapidly hydrolysed at pH's>1.

Taken overall, the results illustrated in Fig. 8 show that Degussa P25 TiO₂ is a better semiconductor photocatalyst for reaction (4) than either of the two WO₃ powders tested, using UV illumination. These findings are not too surprising given the poor reducing power ($E_{CB} = 0.4V$ vs NHE at pH 0) of the photogenerated electrons on WO₃ compared to those on TiO₂ ($E_{CB} = -0.1V$ vs NHE at pH 0). In most cases the more easily dispersed nanocrystalline WO₃ powder performed better than its coarser, microcrystalline counterpart, although not as much as expected based on its much greater specific surface area. Although reasons for this surprisingly modest improvement in activity with increasing specific surface area remain unclear, one possibility is that the nano particulate powder possessed more amorphous character than the microcrystalline powder. Certainly amorphous WO₃, like amorphous TiO₂, has a much lower photocatalytic activity than its crystalline form, since the latter will be associated with a much greater density of defects and such defects are known to be very effective as electron-hole recombination centres and so lower the overall photoefficiency of the semiconductor material.

From the data illustrated in Fig. 8, it is clear that the Ag⁺ ion is the best SEA tested. However, as it results in the photodeposition of Ag onto the surface of the semiconductor particles, and an associated general darkening of the semiconductor powder and permanent alteration of the semiconductor, it is far from ideal as a SEA. Of the other effective SEAs, Ce⁴⁺ and Fe³⁺ ions are both highly UV-absorbing, especially when used at a high concentration, and, given their tendencies to hydrolyse, cannot be used except under quite acidic conditions. Thus, of all the SEAs tested, persulfate appears the best, since it is effective, colourless and can be used over a wide pH range. Indeed, other work shows that it is 6 times more effective at pH 13 compared to the pH used in this work, *i.e.* pH 6.5. Surprisingly, despite the fact that persulfate has proved a very popular SEA in studies of the dye-sensitised oxidation of water, persulfate has hardly been studied as a SEA in the semiconductor-sensitised oxidation of water. Thus, further work is in progress to investigate this process in more detail.

4. Conclusion

In general, the greatest rate of oxygen production was obtained using a TiO₂ semiconductor photocatalyst and silver ions as the sacrificial electron acceptor. However, as alternative SEAs sodium persulfate, iron nitrate and cerium sulphate also appeared effective and resulted in significant rates of oxygen production. Hg²⁺ and Cu²⁺ did not show oxygen production with all the tested semiconductors probably due to a low thermodynamic driving force and highly reactive intermediates that may adsorb on the surfaces of the semiconductors. Sodium persulfate as a SEA in the photo-oxidation of water by semiconductor photocatalysis appears the best of the ones tested and warrants further research.

Acknowledgements

MAV and AM thank IPN and CONACYT for funding a sabbatical year for MAV at Strathclyde University in order to study semiconductor-photocatalysed reactions.

* Corresponding Author. Permanent address: Laboratorio de Catálisis y Materiales, ESQIE-Instituto Politécnico Nacional, Edificio 8, tercer piso, Zacatenco, 07738, Mex, D.F. México., mavalenz@ipn.mx.

1. A. Mills, S.L. Hunte, *J. Photochem. Photobiol. A: Chemistry*, **108** (1997) 1.
2. N. Serpone, A.V. Emeline, *Int. J. Photoenergy*, **4** (2002) 91.
3. A. Fujishima, T.N. Rao, D.A. Tryk, *J. Photochem. Photobiol. C: Photochem. Rev.*, **1** (2000) 1.

4. A.L. Linsebigler, G. Lu, J.T. Yates Jr., *Chem. Rev.*, **95** (1995) 735.
5. M.R. Hoffmann, S.T. Martin, W. Choi, D.W. Bahnemann, *Chem. Rev.*, **95** (1995) 69.
6. M.A. Fox, M.T. Dulay, *Chem. Rev.*, **93** (1993) 341.
7. A.K. Fujishima, K. Hashimoto, T. Watanabe, *TiO₂ Photocatalysis: Fundamental and Applications*, (Bkc, Inc. 2001).
8. M. Kamei, T. Mitsuhashi, *Surf. Sci.*, **L609** (2000) 463.
9. S. Hager, R. Bauer, G. Kudielka, *Chemosphere* **41** (2000) 1219.

10. A. Topalov, D. Molnar-Gabor, M. Kosanic, B. Abramovic, *Water Res.*, **34** (2000) 1473.
11. T.N. Obee, S. Satyapal, *J. Photochem. Photobiol. A: Chem.*, **118** (1988) 45.
12. Z. Huang, P.C. Maness, D.M. Blake, E.J. Wolfrum, S.L. Smolinski, W.A. Jacoby, *J. Photochem. Photobiol. A: Chem.*, **130** (2000) 163.
13. W.A. Jacoby, P.C. Maness, D.M. Blake, E.J. Wolfrum, J.A. Fennell, *Environ. Sci. Tech.*, **32** (1998) 2650.
14. J.C. Ireland, P. Klostermann, E.W. Rice, R.M. Clark, *Appl. Environ. Microbiol.*, **59** (1993) 1168.
15. J.C. Sjogren, R.A. Sierka, *Appl. Environ. Microbiol.*, **59** (1993) 1168.
16. R. Cai, K. Hashimoto, K. Itoh, Y. Kubota, A. Fujishima, *Bull. Chem. Soc. Jpn.*, **64** (1991) 1268.
17. M.I. Litter, *Appl. Catal., B: Environ.*, **23** (1999) 89 and references therein.
18. A.J. Bard, M.A. Fox, *Accts. Chem. Res.*, **28** (1995) 141.
19. A.K. Fujishima, K. Honda, *Nature*, **238** (1972) 37.
20. A.J. Bard, *J. Photochem.*, **10** (1979) 59.
21. J.M. Lehn, in: J.S. Conolly (Ed.), *Photochemical Conversion and Storage of Solar Energy*, (Academic Press, Nueva York, 1981).
22. S. Sato, J.M. White, *J. Catal.*, **69** (1981) 128.
23. A. Harriman, M.A. West (Eds.) *Photogeneration of Hydrogen*, (Academic Press, 1982).
24. A. Mills, G. Porter, *J. Chem. Soc. Faraday Trans. I*, **78** (1982) 3659, y las referencias allí citadas.
25. K. Kalyanasundaram, M. Grätzel, E. Pelizzetti, *Coord. Chem. Rev.*, **69** (1986) 57.
26. M. Shiavello (ed.), *Photocatalysis and Environment, Trends and Applications*, NATO ASI Series, C237, Kluwer Academic Publishers, London (1987).
27. M. Grätzel, *Heterogeneous Photochemical Electron Transfer*, (CRC Press, Boca Raton, 1989).
28. N. Serpone, E. Pelizzetti, *Photocatalysis, Fundamentals and Applications*, (Academic Press, Nueva York, 1989).
29. K. Sayama, H. Arakawa, *J. Phys. Chem.*, **97** (1993) 531.
30. A.J. Bard, M.A. Fox, *Acc. Chem. Res.*, **28** (1995) 141.
31. A. Amouyal, *Solar Ener. Mater. Solar Cells*, **38** (1995) 249.
32. J.R. Bolton, *Solar Energy*, **57** (1996) 37.
33. M. Ashokkumar, *Int. J. Hydrogen Energy*, **23** (1998) 427.
34. K. Fujihara, T. Ohno, M. Matsumura, *J. Chem. Soc. Faraday Trans. 94* (1998) 3705.
35. A. Mills, S.-K. Lee, *Platinum Metal Rev.*, **47** (2003) 2, y las referencias allí citadas.
36. H. Kato, A. Kudo, *Catal. Today*, **78** (2003) 561.
37. T. Takata, A. Tanaka, M. Hara, J.N. Kondo, K. Domen, *Catal. Today*, **44** (1998) 17.
38. A. Mills, S. Morris, *J. Photochem. Photobiol. A: Chem.* **70** (1993) 183.
39. A. Mills, S. Morris, *J. Photochem. Photobiol. A: Chem.* **71** (1993) 75.
40. A. Mills, A. Harriman, G. Porter, *Anal. Chem.*, **53** (1981) 1254.
41. G.R. Bamwenda, K. Sayama and H. Arakawa, *J. Photochem. Photobiol. A: Chem.* **122** (1999) 175.
42. F.A. Cotton and G. Wilkinson, *Advanced Inorganic Chemistry*, 3rd ed., (Interscience, New York, 1972).
43. Y. Tang, R.P. Thorn, R.L. Mauldin and P.H. Wine, *J. Photochem. Photobiol. A: Chem.* **44** (1988) 243.
44. G.R. Bamwenda, T. Uesigi, Y. Abe, K. Sayama and H. Arakawa, *Applied Catal.*, **205** (2001) 117.
45. G.R. Bamwenda and H. Arakawa, *J. Mol. Catal. A: Chem.*, **161** (2000) 105.
46. T. Ohno, F. Tanigawa, K. Fujihara, S. Izumi and M. Matsumura, *J. Photochem. Photobiol. A: Chem.*, **118** (1998) 41.